On the contribution of a hard galactic plane component to the excesses of secondary particles*

Yi-Qing Guo(郭义庆) Hong-Bo Hu(胡红波) Zhen Tian (田珍)

Key Laboratory of Particle Astrophysics, Institute of High Energy Physics, Chinese Academy of Sciences, Beijing 100049, China

Abstract: The standard model of cosmic ray propagation has been very successful in explaining all kinds of galactic cosmic ray spectra. However, high precision measurement have recently revealed an appreciable discrepancy between data and model expectations, from spectrum observations of γ-rays, e^+/e^- and probably the B/C ratio starting from $\sim$10 GeV energy. In this work, we propose that a hard galactic plane component, supplied by the fresh cosmic ray sources and detained by local magnetic fields, can contribute additional secondary particles interacting with local materials. By properly choosing the intensity and spectral index of the harder component up to multi-TeV energy, a two-component γ-ray spectrum is obtained and agrees very well with the observation. Simultaneously, the expected neutrino numbers from the galactic plane could contribute $\sim 60\%$ of IceCube observed neutrino number below a few hundreds of TeV under our model. In addition to these studies, we find that the same pp-collision process responsible for the excess gamma ray emission could account for a significant amount of the positron excess, but a more detailed mechanism is needed for a full agreement. It is expected that the excesses in the $\overline{\rm p}/{\rm p}$ and B/C ratio will show up when energy is above $\sim$10 GeV. We look forward this model being tested in the near future by new observations from AMS02, IceCube, ASγ, HAWC and future experiments such as LHASSO, HiSCORE and CTA.

Keywords: cosmic ray, gamma ray, neutrino

PACS: 03.30.+p, 02.40.-k **DOI:** 10.1088/1674-1137/40/11/115001

1 Introduction

Recent decade has witnessed great progress being made in Cosmic Ray (CR) physics. With the new generation of space-borne and ground-based experiments, CRs are stepping into an era of high precision. PAMELA discovered a clear positron excess for energy between 10—100 GeV in 2009 [1]. Recently, the AMS2 collaboration has released its first result, i.e. the positron fraction $e^+/(e^-+e^+)$ measurement with energy between $\sim$ 0.5 GeV to $\sim$ 350 GeV [2], which confirmed the PAMELA positron excess with unprecedented high precision. These results have stimulated a lot of theoretical studies from the point of view of either exotic processes [3–7] or astrophysics processes [8–11].

Due to the fact that anti-proton excess has not been observed, the contribution to the e^+ excess from the interaction between CRs and InterStellar Medium (ISM) was constrained by the $\overline{\rm p}/{\rm p}$ and B/C ratio [12–16]. High precision observation of diffuse γ-rays obtained by Fermi-LAT shows that a discrepancy between data and model prediction above $\sim$10 GeV is evident [17]. The Fermi-LAT excess actually is consistent with the multi-TeV excess observed by MILAGRO in the inner galactic plane [18] by taking into account the contribution from a Hard Galactic Plane Component (HGPC) [19]. The diffuse γ-ray in the CYGNUS region within tens of degrees observed by Fermi-LAT and MILAGRO [20] is also explainable by HGPC [21]. The continued excess all over the galactic plane and no excess outside the galactic plane does not favor the dark matter interpretation. By considering the fast energy loss, the IC scattering process of electrons is constrained by an earlier study [22]. In short, the diffuse γ-ray excess tends to suggest the existence of the extra CRs, which interact with the ISM.

The neutrino, being only generated from the interaction between CRs and ISM, provide a unique probe to study the origin and acceleration of CRs. Thanks to the IceCube experiment, very high energy neutrino observation has made great progress. The IceCube collaboration reported the detections of two PeV neutrino events and 26 other neutrino events from 30 to 400 TeV with 2 years of data [23, 24]. The number of events exceeds the background by 2.8σ and 3.3σ respectively. Recently updated results with a total number of 37 neutrino events from 30 TeV to 2 PeV corresponding to 5.7σ has been published for 3 years of data combined [25]. By including the TeV energy neutrinos, the spectrum can be described by a

Received 17 September 2015, Revised 28 July 2016

∗ Supported by the Ministry of Science and Technology of China, Natural Sciences Foundation of China (11135010).

©2016 Chinese Physical Society and the Institute of High Energy Physics of the Chinese Academy of Sciences and the Institute of Modern Physics of the Chinese Academy of Sciences and IOP Publishing Ltd

power law with an index of -2.46 [26]. Two types of origins have been discussed in the literatures: galactic and extra-galactic sources. The galactic origins include the TeV γ-ray point sources [30, 31], the galactic center, Fermi bubble region [32–34] and the diffuse CR interaction with the ISM [35–37]. Most recently , Neronov and Semikoz found that both diffuse γ-ray and IceCube neutrino excesses can be well described if the spectral index of galactic CRs is -2.5 [29]. As the HGPC allows a harder spectrum than the one required in [29], its contribution to the IceCube neutrino excesses may not be ignorable.

With all of these high precision results, one can estimate the energy power of the excess particles. For simplicity, we assume that the fluxes of diffuse γ-rays are isotropic on a spherical shell with a distance of 8 kpc from galactic center. According to the integrated flux of diffuse γ-rays above 10 GeV, which is 2.5×10^{-9} ergs $\cdot$ cm$^{-2}\cdot$s$^{-1}\cdot$sr^{-1} [29], the power of excess γ-rays is $\sim 2\times10^{37}$ ergs/s. Similarly, the power of the neutrino excess is estimated to be $\sim 10^{37}$ ergs/s by adopting the IceCube spectra mentioned above and extrapolating the lower energy side to 10 GeV [26, 29]. The power of the positron excess need to be estimated in a different way. Based on the excess positron flux measured by AMS02, its local energy density is $\sim 10^{-5}$ eV. Assuming this is the average value in the galaxy and considering the volume of our galaxy is $\pi(20\text{ kpc})^2(0.2\text{ kpc})\sim10^{67}$cm^3 , the power of excess positron is estimated to be $\sim 4\times10^{36}$ ergs/s if the dominant multi-GeV excess positrons have a lifetime of 10^6 years. It is interesting to notice that the energy power of the three kinds of excess particles is of the same order of magnitude and thus it is natural to ask whether these excesses of γ-rays, neutrinos and positrons share the same origin. If the answer is true, one possible explanation is that one part of the CRs is missed by the steady state solution in the standard model of CR propagation. Following this picture and considering that all excess phenomena happen between ~10 GeV to sub-PeV, the involved CRs must have harder spectra between ~100 GeV to ~PeV.

As a matter of fact, two types of HGPC have been studied widely in the literature. The first type includes point sources and extended sources (the apparent size of the source really depends on its distance and age), where the HGPC is either under or soon after acceleration. According to the diffusive shock acceleration theory, their CRs should have a power law spectrum with an index of about -2. The contributions have been well demonstrated by the γ-ray observations from galactic center [38], Cygnus Cocoon [39, 40] and so on. The second type of HGPC fills the whole galactic disk and is related to the propagation of CRs. As in the simple example proposed by Tomassetti [113], Two Halo diffusion Model (THM) leads to a two component spectrum and could successfully explain the hardening of nuclei spectra at rigidity of ~200 GV observed by ATIC, CREAM and PAMELA [64, 65, 67]. The key point of THM is that the diffusion coefficient has a smaller rigidity dependence in the thin inner halo (i.e., galactic disk) than in the wide outer halo (i.e., traditional galactic halo). The CRs, especially at high energy, stay longer in the disk and contribute an additional harder component. The point of this paper tends to explain the excess of γ-rays at the galactic plane by adopting HGPC. Simultaneously, the γ-rays can be used as a direct probe of the CR densities and spectra in distant locations and can quantify the contribution of the HGPC. The extra hadronic interactions can contribute part of the "excesses" of other secondary particles, such as PAMELA positrons and IceCube neutrinos. Particularly, flatter distributions of $\overline{\rm p}$/p and B/C ratios are expected.

The paper is organized in the following way. Section 2 describes the conventional propagation model of CRs and the additional secondary production from the HGPC interaction with ISM. Section 3 presents the results of the calculation compared with the observation. Finally, Section 4 gives the discussion and conclusion.

2 CR propagation and interactions in the galaxy

Expanding diffusive shocks, generated in the active phase of astrophysical object such as SNRs [42–44] and the galactic center [45–49], are able to accelerate CRs to very high energy. Then these particles would diffuse away from the acceleration site, and travel in the galaxy for $\sim 10^7$ years. The journey involves many processes which are described by the following propagation equation:

$$\begin{aligned}\frac{\partial\psi(\vec{r},p,t)}{\partial t}=&q(\vec{r},p,t)+\vec{\nabla}\cdot\left(D_{xx}\vec{\nabla}\psi-\vec{V}_c\psi\right)\\&+\frac{\partial}{\partial p}p^2D_{pp}\frac{\partial}{\partial p}\frac{1}{p^2}\psi\\&-\frac{\partial}{\partial p}\left[\dot{p}\psi-\frac{p}{3}\left(\vec{\nabla}\cdot\vec{V}_c\psi\right)\right]\\&-\frac{\psi}{\tau_f}-\frac{\psi}{\tau_r}\end{aligned}\tag{1}$$

where $\psi(\vec{r},p,t)$ is the density of CR particles per unit momentum p at position $\vec{r}$, $q(\vec{r},p,r)$ is the source distribution, D_{xx} is the spatial diffusion coefficient, $\vec{V}_{\rm c}$ is the convection velocity, D_{pp} is the diffusion coefficient in momentum space and is used to describe the reacceleration process, $\dot{p}\equiv{\rm d}p/{\rm d}t$ is momentum loss rate, and τ_f and τ_r are the characteristic time scales for fragmentation and radioactive decay respectively. Conventionally, the spatial diffusion coefficient is assumed to be space-independent and has a power law form $D_{xx}=\beta D_0(\rho/\rho_0)^\delta$ of the rigidity ρ, where δ reflects the prop-

erty of the ISM turbulence. The re-acceleration can be described by the diffusion in momentum space and the momentum diffusion coefficient D_{pp} is coupled with the spatial diffusion coefficient D_{xx} as [50]

$$D_{pp}D_{xx} = \frac{4p^2v_{\rm A}^2}{3\delta(4-\delta^2)(4-\delta)w} \quad (2)$$

where $v_{\rm A}$ is the Alfven speed, and w is the ratio of magnetohydrodynamic wave energy density to the magnetic field energy density, which can be fixed to 1. The CRs propagate in an extended halo with a characteristic height $z_{\rm h}$, beyond which free escape of CRs is assumed. The values of the key parameters of CR propagation are listed in Table 1, which is similar to previous studies except for the tuned injection spectrum [5, 51–53]. Detailed studies of the uncertainties about the conventional model can be found in Refs. [54–56].

Table 1. Propagation parameters.

$D^0/(10^{28}\ {\rm cm}^2\cdot{\rm s}^{-1})$	5.5	ρ_0/GV	4
δ	0.45	$v_{\rm A}/{\rm km}\cdot{\rm s}^{-1})$	32
$R_{\rm max}$/kpc	20	$z_{\rm h}$/kpc	4

It is generally believed that SNRs are the sources of galactic CRs. The spatial distribution of SNRs is usually described by following empirical formula:

$$f(r,z) = \left(\frac{r}{r_\odot}\right)^a \exp\left(-b\cdot\frac{r-r_\odot}{r_\odot}\right)\exp\left(-\frac{|z|}{z_s}\right), \quad (3)$$

where $r_\odot = 8.5$ kpc is the distance from the Sun to the galactic center, $z_s \approx 0.2$ kpc is the characteristic height of galactic disk, and a=1.25 and b=3.56 are adopted from [57], which are suggested from Fermi-LAT studies on diffuse γ-ray emission in the 2nd galactic quadrant [58]. The accelerated spectrum of primary CRs at the source region is assumed to be a broken power law function:

$$q^i(p) = q_0^i \times \begin{cases} (p/p_{\rm br})^{-\nu_1} & \text{if } (p < p_{\rm br}), \\ (p/p_{\rm br})^{-\nu_2}\cdot f(\hat{p}) & \text{if } (p \geqslant p_{\rm br}) \end{cases} \quad (4)$$

where i denotes the species of all nuclei and electron, p is the rigidity, and q_0^i is the normalization factor for all nucleus and electron, relative abundance of each nuclei follows the default value in the GALPROP package [59]. $p_{\rm br}$ is the broken energy and ν_1, ν_2 is the spectrum index before and after the broken energy $p_{\rm br}$. $f(\hat{p})$ is used to describe the high energy cut-off and $\hat{p}$ is the break rigidity. For the primary electrons, a soft spectrum index with the value of -3.5 at the rigidity 2 TV is adopted in order to agree with HESS observations [61]. For the nuclei, to reproduce the knee structure of CRs, $f(\hat{p})$ can be described as the following formula based on the Hörandel model [62]:

$$f(p_{\rm knee}) = \left[1+\left(\frac{p}{\hat{p}}\right)^{\epsilon_{\rm c}}\right]^{\frac{-\Delta\gamma}{\epsilon_{\rm c}}} \quad (5)$$

where $\Delta\gamma$ and $\epsilon_{\rm c}$ characterize the change in the spectrum at the break rigidity $\hat{p}$. Detailed information of the parameters is listed in Table 2.

Table 2. The injection spectrum of primary CRs.

parameters	nuclei	electron
$\log(q_0^i)$	-8.31	-9.367
ν_1	1.92	1.5
ν_2	2.31	2.7
$p_{\rm br}$/GV	9	5.7
$\hat{p}$/PV	3.68	
$\Delta\gamma$	0.44	
$\epsilon_{\rm c}$	1.84	

When the low energy CRs arrive at the solar environment, the direction of motion will be affected by the solar wind. This is called solar modulation. The force-field approximation is used to describe the solar modulation by the modulation potential Φ [60]. In this work, the modulation potential Φ is fixed as Φ=550 MV for proton and anti-proton, Φ=300 MV for B/C, Φ=600 MV for positron and electron, as discussion Ref. [52].

By using the publicly available numerical code GALPROP and by taking the main parameters described above, the directly measured proton spectrum up to ~100 TeV can be successfully reproduced as shown in Fig.1. Simultaneously, the calculation can provide all spectra of observable secondary particles for comparison with the experimental results. We will refer to those results from the corresponding calculation as conventional model results hereafter.

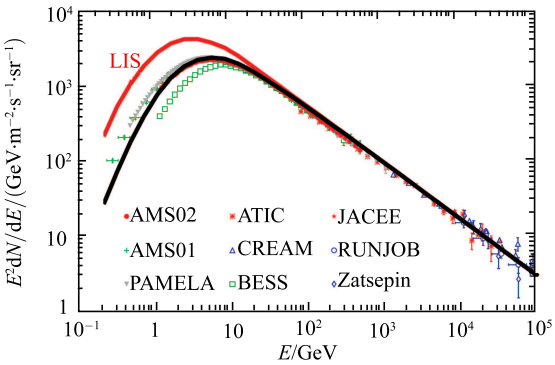

Fig. 1. (color online) The proton spectrum in the conventional model as shown by the solid red line before considering solar moduation and by the solid black line after considering solar moduation. The experiment data for protons come from: AMS02 [63], ATIC [64], PAMELA [65], AMS01 [66], CREAM [67], BESS [68], JACEE [69], RUNJOB [70], Zatsepin [71].

Conventional model calculations are able to describe well the high latitude diffuse γ-ray spectra but do not give a good enough description of the spectra in the

galactic plane [17]. Distributed along the galactic disk, the HGPC has been discussed and expected to resolve the deficit problem [21, 29]. The ideal way to incorporate the effects of HGPC is to include all these details in the calculation of the propagation equation, including the temporal variant injection spectra, the spatial dependent discrete source distribution, the diffusion coefficient and so on. As a first-order approximation, this work focuses only on the averaged production of secondary CRs by the HGPC and does not attempt to understand the individual contributions of the HGPC. For this purpose, an effective description of the HGPC offers an alternative approach. To some extent, this is actually an exact approach. In other words, one effective term for the HGPC could account for all the contributions from point sources and extended sources in the galactic disk.

In this work, we assume that the HGPC has the same spatial distribution as that of the SNRs and stays in this region. It means that the HGPC does not take part in the propagation as the primary or secondary particles do. Furthermore, the spectum of the HGPC should be close to the injected spectrum of primary CRs. In fact, we simply employ the injected spectrum of primary CRs as in Formula 4, but with a rescaled normalization factor. The rescaled normalization factor is actually a free parameter and determined by giving the best agreement between the model calculation and observations.

3 Results on secondary particle spectra

Base on the above discussion, the secondary particles are produced from two components: steady state CRs in the conventional model and the HGPC. The secondary spectra from the contribution of the conventional model can be directly obtained from the GALPROP package calculation. The secondary particle production from the HGPC is calculated under the GALPROP frame work by switching off the propagation of HGPC to keep the HGPC spectrum unchanged and limit the related interactions only in the source region. After the production, the secondary particles follow the same propagation as those from the conventional model calculation. In which, the spectra of additional secondary particles can be obtained. Given a rescaled normalization factor, the summed spectra of secondary particles can be compared with the observations. By adjusting the rescaled normalization factor, we find that a value of 0.4 offers the best agreement.

3.1 Diffuse γ-ray emission

The diffuse γ-rays in the galactic plane are produced through three major processes: decay of π^0 generated by pp-collisions, IC scattering off the ISRF and bremsstrahlung by electrons. In the case of IC calculation, the widely used ISRF model is adopted [72, 73].

According to the available spectra of high energy diffuse γ-rays on the galactic disk, four regions are studied in this work: (a) Inner Most Galactic Plane(IMGP:$|b| < 5^\circ$ & $|l| < 30^\circ$), (b) Inner Galactic Plane (IGP:$|b| < 8^\circ$ & $|l| < 80^\circ$), (c) Outer Galactic Plane (OGP:$|b| < 8^\circ$ & $|l| > 80^\circ$) and (d) Cygnus Region(CygR). Figure 2 (a)—(c) show the comparisons of the diffuse γ-rays from region (a)—(c). All of our conventional model calculations agree well with those from the Fermi-LAT collaboration [17]. The general conclusion is that model calculation can not describe the observation with the energy above a few GeV. After adding the contribution from the HGPC, also dominated by π^0 decay, the agreement between model calculations and observations is much better from 1 to 100 GeV.

The hard spectrum is expected to continue to very high energy due to the HGPC contribution, which can be tested by diffuse γ-ray obsevation at higher energy. Fortunately, multi-TeV observation has been performed by ground-based EAS experiments in CygR. Figure 2 (d1) show the spectrum observed by Fermi-LAT in a wide CygR region together with model calculations. Though HGPC helps to explain the observation above 10GeV, the overall theoretical spectrum underestimates the Fermi-LAT observation. This is probably because CygR is a star formation region which contains many accelerators, old and young. A full understanding should take into account all contributions, including those from point sources and extended sources. Another possibility is that the ISM in this region is not properly modeled in the calculation; if we increase the amount of gas by 25%, the calculation can have perfect agreement with observation. ARGO-YBJ performed TeV observation in a slightly different area in CygR as shown in Fig. 2 (d2). The calculated flux agrees with the observation within experimental error. However, the measured flux has a large uncertainty and precision tests are clearly foreseen with new observations from Tibet-ASγ [74] and HAWC [75]. Figure 2 shows the spectra meaurement by EGRET and MILAGRO from a narrow band of CygR along the galactic plane. Model calculation shows very good agreement with the observations from sub-GeV to tens of TeV energy. The HGPC contributes almost all the γ-ray emission at multi-TeV energy. More accurate observations of diffuse γ-rays above multi-TeV energy will be crucial in testing the HGPC hypothesis.

3.2 Diffuse neutrino emission

Charged pion decay will produce neutrinos accompanied by γ-rays. Different from γ-ray observations, neutrinos interact very weakly with matter and a very large

volume of target material is required to detect the neutrino events.

With a cubic kilometer ice telescope below the surface of the South Pole, the IceCube collaboration reported a detection of 37 neutrino candidate events from 30 TeV to 2 PeV, with a background of 8.4±4.2 from CR muon events and $6.6^{+5.9}_{-1.6}$ from atmospheric neutrinos during a lifetime of 988 days [25]. By including TeV measurement, the neutrino spectrum is obtained from ∼TeV to ∼PeV energy [26]. The left panel of Fig. 3 shows the IceCube data points together with the model calculation. It can be seen that the theoretical calculation of allsky flux as shown by the black solid line is lower than the experimental observation. The best-fit result, shown by the gray solid line, indicates that the HGPC contributes ∼60% of the IceCube observation. It should be noted that the galactic neutrino flux mainly come from galactic plane according to our model calculation as shown in the right panel of Fig. 3 by the black solid line. This conclusion apparently contradicts that of the IceCube collaboration, which claimed an isotropic distribution based on the current limited number of neutrino events. It is possible that the extrapolation of the hard component to ∼ PeV is unlikely to be the right approach, which may overestimate the galactic contribution. According to our previous work [37], the galactic contribution of neutrino flux is expected to be at the level of 10% by adopting the flux of CRs from the conventional model.

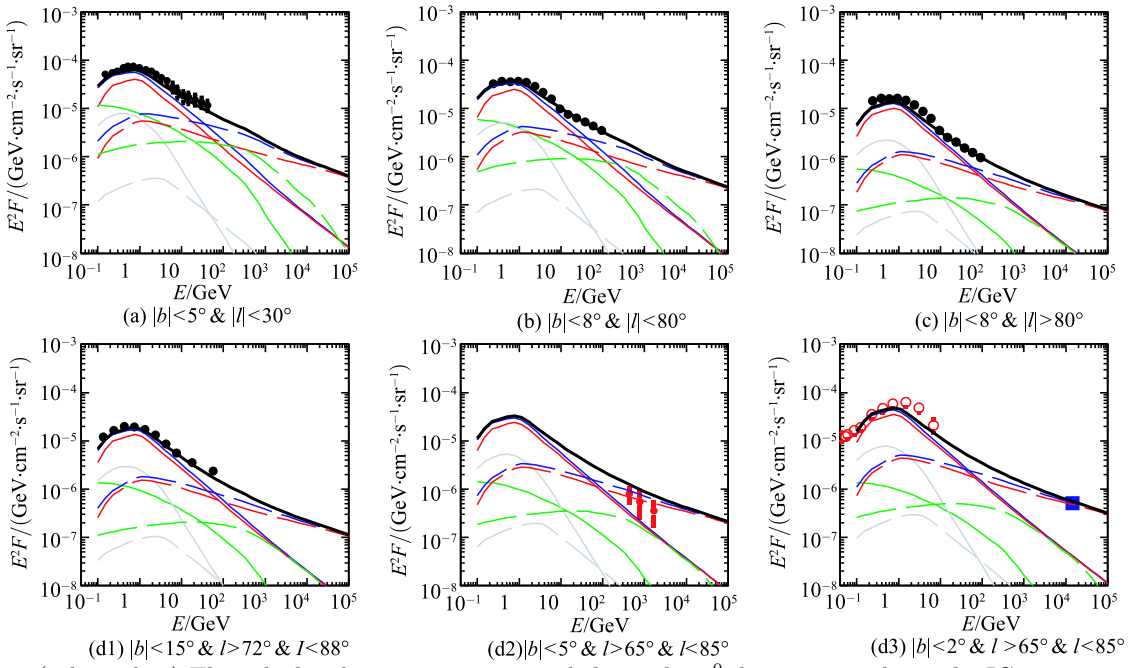

Fig. 2. (color online) The calculated γ-ray spectrum: red shows the π^0 decay, green shows the IC scattering, gray shows the bremsstrahlung process and black shows the total spectrum; here solid lines represent the contribution from the conventional model and dashed lines represent the contribution from the HGPC. The data at GeV energy range with black circles is from Fermi-LAT [17, 20, 27, 76] and that with red open circles is from EGRET [77]. The data at TeV energy range with red points is from the ARGO experiment [78]; the data at 15 TeV energy with blue squre points is from the MILAGRO experiment [18].

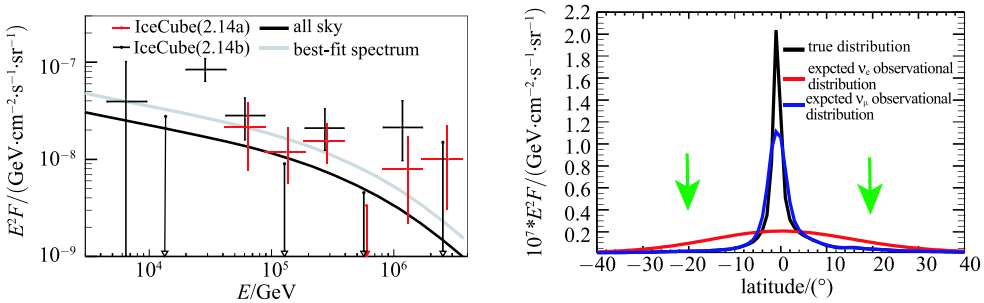

Fig. 3. (color online) The calculated diffuse neutrino spectrum(left panel) from collision of CRs with ISM. The data is astrophysical neutrino observations [25, 26]. The right panel is the integrated neutrino flux for $E > 30$ TeV along l=0. The black line is the true distribution in our model and the red is the reconstructed distribution for $\nu_e(\nu_\mu)$ after considering the angular resolution of 15°(1.5°).

3.3 The ratio of $\overline{\mathrm{p}}$/p and B/C

There is great astrophysical interest in CR antiprotons and boron nuclei. It is believed that most of antiprotons and boron nuclei originate from collisions of CRs with ISM. Therefore information about CR propagation can be extracted from comparison between the spectra of secondary particles and those of primary CRs. Based on the above discussion, the diffuse γ-ray excess, and part of the IceCube neutrinos can be explained by the HGPC. There is no doubt that antiprotons and boron nuclei as secondary particles should be expected to have excesses for energy above tens of GeV.

The left panel of Fig. 4 shows the calculated $\overline{\mathrm{p}}$/p and the right panel shows the B/C. The blue and red dashed lines present the calculated results from conventional and HGPC models respectively. The black solid line gives the total contribution. With considering the contribution of the HGPC, the overall calculation on the ratio of $\overline{\mathrm{p}}$/p is a little higher than the PAMELA observation [79, 80]. However, the uncertainty of $\overline{\mathrm{p}}$ production cross section is $\sim 25\%$ in the energy range 0.1—100 GeV [81, 82], which should lead to the same level of uncertainty in the ratio calculation. Taking all of these factors into account, the model calculation is consistent with the observation within the errors. On the other hand, the ratio of B/C is quite consistent with the AMS02 observation after considering the HGPC contribution. Owing to its hard spectrum, the HGPC induced secondary $\overline{\mathrm{p}}$ and boron nuclei inherit a similar hard spectrum, which make the ratio of $\overline{\mathrm{p}}$/p, B/C considerably flatter than that from conventional model. Such a tendency is not obvious in current observations. In the future, high statistics and TeV energy observation can offer a crucial and definitive identification of this model.

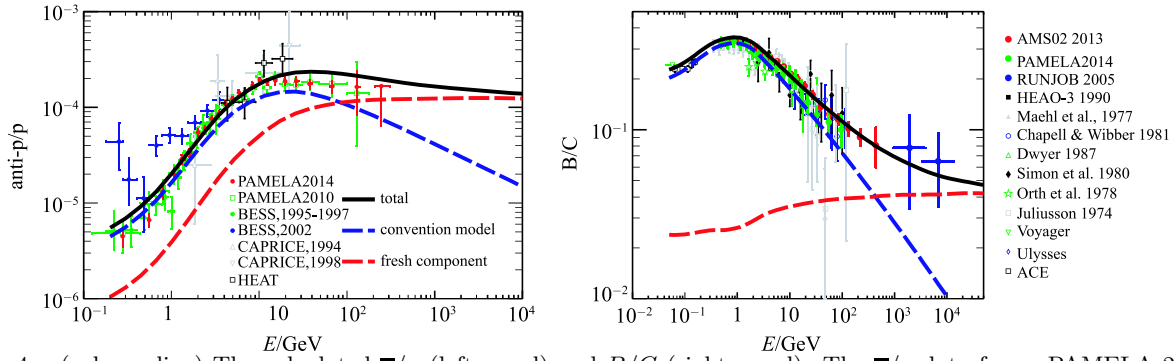

Fig. 4. (color online) The calculated $\overline{\mathrm{p}}$/p (left panel) and B/C (right panel). The $\overline{\mathrm{p}}$/p data from: PAMELA 2014 [80], PAMELA 2010 [79], BESS 1995-1997 [83], BESS 1999 [84], CAPRICE 1994 [85], CAPRICE 1998 [86], HEAT [87]. The B/C data from: AMS02 [88], PAMELA [89], RUNJOB [90], Juliusson [91], Dwyer [92], Orth [93], Simon [94], HEAO-3 [95], Maehl [96], Voyager [97], Ulysses [98], ACE [99] and for other references see [100].

3.4 Positron and Electron Excess

Charged pion decay will produce e^+e^- accompanied by neutrinos. In this section, the contribution of secondary particle e^+e^- from the HGPC interaction with ISM will be discussed.

The left panel of Fig. 5 shows the positron spectra from two contributions. The blue and red dashed lines stand for the conventional model and HGPC calculations. Because of the energy loss during the propagation of positron, the resulting spectrum of positrons from

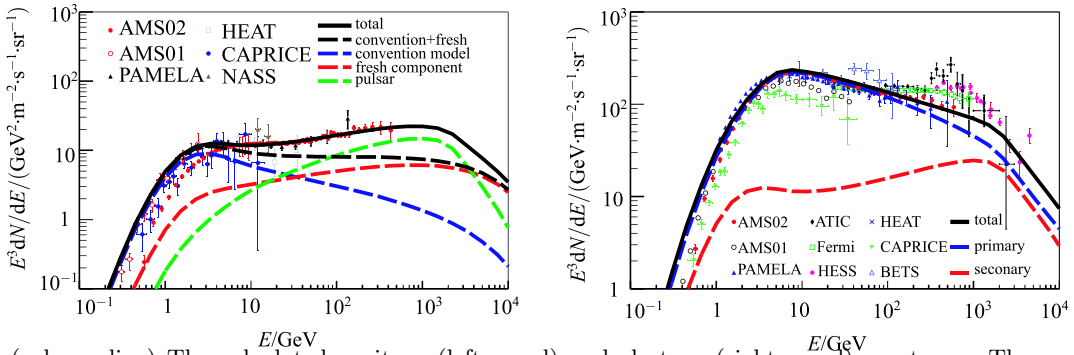

Fig. 5. (color online) The calculated positron (left panel) and electron (right panel) spectrum. The experiment datas are adopted from AMS02 [101], AMS01 [102], PAMELA [1, 103], HEAT [104], CAPRICE [105], ATIC [106], Fermi-LAT [107], HESS [61] and BETS [108].

the HGPC becomes softer, which makes the sum of the two contributions not sufficient for the explanation of the positron excess as shown by the black dashed line. Pulsar sources or exotic physical processes are required to account for the discrepancy. According to the pulsar model [52], the positron spectrum from pulsars can be described by formula 4. Combining the three types of components, the total calculation agrees well with the AMS02 observation as shown by the black solid line.

The right panel of Fig. 5 contains the spectrum of electrons from observations and calculations. The blue dashed line is for the primary electrons from the acceleration sources and the red dashed line is the sum of the three contributions for the case of positrons. In total, they agree with the spectra measured by PAMELA and AMS02 as shown by the black solid line.

Because of the good agreement between the model calculation and observation for both positron and electron spectra, the ratio of positrons to electrons is described very well by our model as shown in Fig. 6.

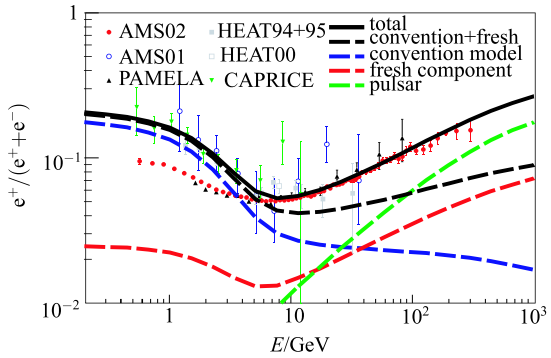

Fig. 6. (color online) The calculated positron fraction. The experiment datas are adopted from AMS02 [2], AMS01 [109], PAMELA [1], HEAT94+95 [110], HEAT00 [111] and CAPRICE [105].

4 Discussion and conclusion

The origin, acceleration and propagation are the fundamental problems of CR physics. In an era when high precision and multi-messenger observation results are floodng in, when various excesses and new phenomena continually pop up, the successful standard model of CRs is facing stringent testing and refinement. By simply adding a HGPC to account for the additional secondary particles production, the diffuse γ-ray excess from 10 GeV to multi-TeV energy can be successfully explained. The same process can generate additional neutrinos and about half of the Ice Cube neutrino flux can be explained. However, just like diffuse γ-rays, these diffuse neutrinos lie on the galactic plane and have a high level of anisotropic distribution. To fully understand the isotropic Ice Cube neutrino, extra-galactic contribution is inevitable. Though the HGPC can generate right amount of electron and positron, but they are still not able to explain the total electron and positron excess simply because of the energy loss on the journey of propagation. If electrons and positrons can undergo fast diffusion with less energy loss, it is expected that the excesses are fully contributed by the HGPC. In the current scenario, electron and positron contribution from astrophysical sources such as pulsars is necessary. A very important difference between pulsars and the HGPC is that the latter model predicts additional production for all secondary particles, including anti-protons and boron nuclei. According to our calculations, the ratio of $\overline{\mathrm{p}}$/p and B/C will become flatter for energy above tens of GeV. High precision observation of flat ratios from AMS02 will be the smoking gun to test the HGPC model [112].

As proposed by earlier work, one possibility was that the HGPC comes from point-like and extended sources [11, 21, 41]. This work is also based on such a picture. Another possibility is related to the propagation of CRs. As in the simple example proposed by Tomassetti [113], Two Halo diffusion Model (THM) leads to a two component spectrum. The key point of the THM is that the diffusion coefficient has a smaller rigidity dependence in the thin inner halo (i.e., galactic disk) than in the wide outer halo (i.e., traditional galactic halo). The HGPC, especially in its high energy part, contributes an additional harder component. Further theoretical study is needed probably under the frame work of DRAGON by adopting a spatially dependent diffusion coefficient [114–116].

We thank XiaoJun Bi and Qiang Yuan for helpful discussion.

References

1 O. Adriani et al, Nature, **458**: 607–609 (2009)
2 M. Aguilar et al, Phys. Rev. Lett., **110**: 141102 (2013)
3 L. Bergström, T. Bringmann, and J. Edsjö, Phy. Rev. D, **78**: 103520 (2008)
4 V. Barger, W. Y. Keung, D. Marfatia, and G. Shaughnessy, Phys. Lett. B, **672**: 141–146 (2009)
5 P. F. Yin, Q. Yuan, J. Liu et al, Phy. Rev. D, **79**: 023512 (2009)
6 J. Zhang, X. J. Bi, J. Liu et al, Phy. Rev. D, **80**: 023007 (2009)
7 P. S. Bhupal Dev, D. K. Ghosh, N. Okada, and I. Saha, arXiv1307.6204
8 H. Yüksel, M. D. Kistler, and T. Stanev, Phys. Rev. Lett., **103**: 051101 (2009)
9 D. Hooper, P. Blasi, and P. Dario Serpico, 2009, JCAP, **1**: 25

(2009)
10 H. B. Hu, Q. Yuan, B. Wang et al, ApJ, **700**: L170–L173 (2009)
11 P. Blasi, Phys. Rev. Lett., **103**: 051104 (2009)
12 O. Adriani et al, Phys. Rev. Lett., **102**: 051101 (2009)
13 P. Blasi and P. D. Serpico, Phys. Rev. Lett., **103**: 081103 (2009)
14 P. Mertsch and S. Sarkar, Phys. Rev. Lett., **103**: 081104 (2009)
15 M. Ahlers, P. Mertsch, and S. Sarkar, Phys. Rev. D, **80**: 123017 (2009)
16 P. Mertsch and S. Sarkar, Phys. Rev. D, **90**: 061301 (2014)
17 M. Ackermann et al, ApJ, **750**: 3 (2012)
18 A. A. Abdo et al, ApJ, **688**: 1078–1083 (2008)
19 H. J. Völk and E. G. Berezhko, ApJ, **777**: 149 (2013)
20 M. Ackermann et al, A&A, **538**: 71 (2012)
21 X. J. Bi, T. L. Chen, Y. Wang, and Q. Yuan, ApJ, **695**: 883 (2009)
22 A. M. Atoyan, F. A. Aharonian, and H. J. Völk, Phys. Rev. D, **52**: 3265–3275 (1995)
23 M. G. Aartsen et al, Phys. Rev. Lett., **111**: 021103 (2013)
24 IceCube Collaboration, Science, **342**: 1 (2013)
25 M. G. Aartsen et al, Phys. Rev. Lett., **113**: 101101 (2014)
26 M. G. Aartsen et al, arXiv:1410.1749
27 A. A. Abdo et al, Phys. Rev. Lett., **104**: 101101 (2010)
28 M. Ackermann et al, arXiv:1410.3696
29 A. Neronov and D. Semikoz, arXiv:1412.1690
30 D. B. Fox, K. Kashiyama, and P. Mészarós, ApJ, **774**: 74 (2013)
31 A. Neronov, D. Semikoz, and C. Tchernin, Phys. Rev. D, **89**: 103002 (2014)
32 S. Razzaque, Phys. Rev. D, **88**: 081302 (2013)
33 M. Ahlers and K. Murase, arXiv:1309.4077
34 M. Su, T. R. Slatyer, and D. P. Finkbeiner, ApJ, **724**: 1044 (2010)
35 N. Gupta, APh, **48**: 75 (2013)
36 J. C. Joshi, W. Winter, and N. Gupta, MNRAS, **439**: 3414 (2014)
37 Y. Q. Guo, H. B. Hu, Q. Yuan, Z. Tian, and X. J. Gao, ApJ, **795**: 100 (2014)
38 F. Aharonian et al, Nature, **439**: 695 (2006)
39 M. Ackermann et al, Science, **334**: 1103 (2011)
40 B. Bartoli, et al, ApJ, **790**: 152 (2014)
41 Y. Fujita, K. Kohri, R. Yamazaki, and K. Ioka, Phys. Rev. D, **80**: 3003 (2009)
42 A. R. Bell, MNRAS, **182**: 147 (1978)
43 A. R. Bell, MNRAS, **182**: 443 (1978)
44 R. D. Blandford and J. P. Ostriker, ApJ, **221**: 29 (1978)
45 V. S. Ptuskin and Y. M. Khazan, AZh., **58**: 959 (1981)
46 S. S. Said, A. W. Wolfendale, M. Giler, and J. Wdowczyk, ICRC, **2**: 344 (1981)
47 M. Giler, JPhG., **9**: 1139 (1983)
48 Y. Q. Guo, Z. Y. Feng, Q. Yuan, C. Liu, and H. B. Hu, NJPh., **15**: 3053 (2013)
49 Y. Q. Guo, Q. Yuan, C. Liu, and A. F. Li, JPhG., **40**: 3053 (2013)
50 E. S. Seo and V. S. Ptuskin, ApJ, **431**: 705 (1994)
51 J. Zhang, Q. Yuan, and X. J. Bi, ApJ, **720**: 9 (2010)
52 Q. Yuan et al, APh, **60**: 1 (2015)
53 S. J. Lin, Q. Yuan, and X. J. Bi, arXiv:1409.6248
54 D. Mauro, F. Donato, R. Lineros, and A. Vittino, JCAP, **4**: 6 (2014)
55 H. B. Jin, Y. L. Wu, and Y. F. Zhou, JCAP, **9**: 49 (2015)
56 G. Giesen, M. Boudaud, Y. Génolini et al, JCAP, **9**: 23 (2015)
57 R. Trotta et al, ApJ, **729**: 106 (2011)
58 L. Tibaldo and I. A. Grenier arXiv:0907.0312
59 A. W. Strong and I. V. Moskalenko, ApJ, **509**: 212 (1998)
60 L. J. Gleeson and W. I. Axford, ApJ, **154**: 1011 (1968)
61 F. Aharonian et al, Phys. Rev. Lett., **101**: 261104 (2008)
62 J. R. Hörandel et al, APh, **21**: 241 (2004)
63 C. Consolandi et al, arXiv:1402.0467
64 A. D. Panov et al, astro.ph.12377 (2006)
65 O. Adriani et al, Science, **332**: 69 (2011)
66 J. Alcaraz et al, Phys. Lett. B, **472**: 215 (2000)
67 H. S. Ahn et al, ApJ, **714**: 89 (2010)
68 T. Sanuki et al, ApJ, **545**: 1135 (2000)
69 K. Asakimori et al, ApJ, **502**: 278 (1998)
70 A. V. Apanasenko, et al, APh, **16**: 13 (2001)
71 J. R. Höorandel, JPhCS, **47**: 41 (2006)
72 A. W. Strong, I. V. Moskalenko, and O. Reimer, ApJ, **537**: 763 (2000)
73 T. A. Porter and A. W. Strong, ICRC, **4**: 77 (2005)
74 S. K. Sako et al, APh, **32**: 177 (2009)
75 A. U. Abeysekara et al, APh, **50**: 26 (2013)
76 O. Macias and C. Gordon, Phys. Rev. D, **89**: 063515 (2014)
77 S. D. Hunter et al, ApJ, **481**: 205 (1997)
78 G. Di Sciascio and IJMPD, **23**: 1430019 (2014)
79 O. Adriani et al, Phys. Rev. Lett., **105**: 121101 (2010)
80 O. Adriani et al, Physics Reports, **544**: 323 (2014)
81 F. Donato et al, ApJ, **563**: 172 (2001)
82 F. Donato et al, Phys. Rev. Lett., **102**: 071301 (2009)
83 S. Orito et al, Phys. Rev. Lett., **84**: 1078 (2000)
84 Y. Asaoka et al, Phys. Rev. Lett., **88**: 051101 (2002)
85 M. Boezio et al, **487**: 415 (1997)
86 M. Boezio, ApJ, **561**: 787 (2001)
87 A. S. Beach et al, Phys. Rev. Lett., **87**: 271101 (2001)
88 M. Aguilar, CERN Courier, **53**: 8 (2013)
89 O. Adriani et al, ApJ, **791**: 93 (2014)
90 V. A. Derbina et al, ApJ, **628**: 41 (2005)
91 E. Juliusson, ApJ, **191**: 331 (1974)
92 R. Dwyer, ApJ, **224**: 691 (1978)
93 C. D. Orth, A. Buffington, G. F. Smoot, and T. S. Mast, ApJ, **226**: 1147 (1978)
94 T. Simon, J. L. Linsky, and III F. H. Schiffer, ApJ, **239**: 911 (1980)
95 J. J. Engelmann et al, A&A, **233**: 96 (1990)
96 R. C. Maehl, J. F. Ormes, A. J. Fisher, and F. A. Hagen, Ap&SS, **47**: 163 (1977)
97 A. Lukasiak, ICRC, **3**: 41 (1999)
98 M. A. Duvernois, J. A. Simpson, and M. R. Thayer, A&A, **316**: 555 (1996)
99 A. J. Davis et al, AIPC, **528**: 421 (2000)
100 S. A. Stephens and R. E. Streitmatter, ApJ, **505**: 266 (1998)
101 M. Aguilar et al, Phys. Rev. Lett., **113**: 121102 (2014)
102 J. Alcaraz et al, Phys. Lett. B, **484**: 10 (2000)
103 O. Adriani et al, Phys. Rev. Lett., **106**: 201101 (2011)
104 S. W. Barwick et al, ApJ, **498**: 779 (1998)
105 M. Boezio et al, ApJ, **532**: 653
106 J. Chang et al, Nature, **456**: 362 (2008)
107 M. Ackermann et al, Phys. Rev. D, **82**: 092004 (2010)
108 S. Torii et al, ApJ, **559**: 973 (2001)
109 M. Aguilar et al, Phys. Lett. B, **646**: 145 (2007)
110 S. W. Barwick et al, ApJ, **482**: 191 (1997)
111 S. Coutu et al, ICRC, **5**: 1687 (2001)
112 G. Giesen et al, arXiv:1504.04276
113 N. Tomassetti, ApJ, **752**: 13 (2012)
114 C. Evoli, D. Gaggero, D. Grasso, and L. Maccione, JCAP, **10**: 18 (2008)
115 D. Gaggero, L. Maccione, G. Di Bernardo, C. Evoli, and D. Grasso, Phys. Rev. Lett., **111**: 021102 (2013)
116 C. Jin, Y. Q. Guo and H. B. Hu, arXiv:1504.06903